Journal of Alloys and Compounds 509 (2011) 5931–5934

Contents lists available at ScienceDirect

Journal of Alloys and Compounds

journal homepage: www.elsevier.com/locate/jallcom

Anisotropic magnetocaloric effect in TbNiAl

J. Kaštil*, P. Javorský, J. Pospíšil

Charles University, Faculty of Mathematics and Physics, Department of Condensed Matter Physics, Ke Karlovu 5, 121 16 Prague 2, Czech Republic

ARTICLE INFO

Article history:
Received 7 January 2011
Received in revised form 27 January 2011
Accepted 1 February 2011

PACS:
75.30.Sg
75.30.Gw

Keywords:
Magnetocaloric effect
TbNiAl
Magnetism
Anisotropy

ABSTRACT

We present study of the anisotropic magnetocaloric effect in TbNiAl crystallizing in the hexagonal ZrNiAl-type structure. TbNiAl orders antiferromagnetically below $T_N = 47$ K and undergoes second magnetic phase transition to another antiferromagnetic structure at $T_1 = 23$ K. Magnetization and specific heat measurements on single crystal revealed strongly anisotropic magnetocaloric effect. The large effect occurs for field applied along the hexagonal *c*-axis whereas the entropy change is almost zero for the perpendicular field direction. Plateau-like character of the determined temperature change is observed between T_N and T_1.

1. Introduction

Magnetic refrigeration techniques based on the magnetocaloric effect (MCE) represent a promising alternative to conventional gas compression technology and other cooling technologies in different temperature regions. The magnetocaloric effect is characterized by the isothermal entropy change ΔS or adiabatic temperature change ΔT when varying external magnetic field. The very broad discussion of different aspects of the magnetocaloric effect can be found e.g. in work of de Oliveira and von Ranke [1] and book of Tishin and Spichkin [2]. The search for better working substances is essential for further improvements of magnetic refrigeration. One of the promising ways is based on employing anisotropic properties of the magnetic refrigerant [3–6]. Large MCE can be associated with rapid changes of either the anisotropy energy or the angle of the magnetization vector. It is also known that the ΔS measured with the magnetic field applied along the easy magnetization direction is remarkably larger than that along the hard direction [7]. Considerable MCE in some material can be thus achieved only rotating the crystal, from the hard to the easy magnetization direction without changing the applied magnetic field. The magnetic entropy change due to this rotation is equal to the difference of entropy change caused by the field applied along the hard and easy directions.

As the large MCE occurs at temperatures around the magnetic phase transitions, the characterization of magnetocaloric materials generally becomes associated with a detailed study of the nature of these phase transitions and the magnetic order, which is also interesting from a fundamental point of view. The *R*NiAl compounds exhibit complex magnetic properties with multiple phase transitions. The presence of multiple phase transitions can be generally of high importance in the search of materials showing table-like MCE. Very broad temperature region with large entropy change was observed and widely discussed in (Gd,Er)NiAl compounds [8]. As inferred from magnetization measurements on polycrystalline samples, large MCE exhibits also other *R*NiAl compounds: DyNiAl [9], HoNiAl [10] and TbNiAl [11]. All these *R*NiAl compounds crystallize in the layered hexagonal ZrNiAl-type structure, which suggests possibility of a strong magnetocrystalline anisotropy as observed e.g. in all uranium compounds with this crystal structure [12]. Strongly anisotropic MCE was really recently observed on DyNiAl single crystal [13]. In this work, we focus on TbNiAl which exhibits the strongest uniaxial magnetocrystalline anisotropy among the *R*NiAl series [14]. The neutron diffraction measurements revealed that TbNiAl orders antiferromagnetically with the propagation vector $(1/2\,0\,1/2)$ below $T_N = 47$ K and undergoes second magnetic phase transition to another antiferromagnetic structure at $T_1 = 23$ K [14,15]. The triangular arrangement of Tb atoms within the basal planes causes a geometrical frustration of 1/3 of the Tb magnetic moments between T_N and T_1. The frustrated moments change the propagation at T_1 leading to magnetic structure where all Tb moments have the same magnitude at 2 K. All the magnetic

* Corresponding author.
E-mail addresses: jirka.kastil@centrum.cz, jirka.kastil@gmail.com (J. Kaštil).

0925-8388/$ – see front matter © 2011 Elsevier B.V. All rights reserved.
doi:10.1016/j.jallcom.2011.02.001

moments are aligned along the hexagonal *c*-axis in both magnetic phases [14,15]. The metamagnetic transition to collinear ferromagnetic order occurs in magnetic field of B_{crit} = 0.4 T applied along the *c*-axis. The magnetization data point to very strong uniaxial magnetocrystalline anisotropy with the anisotropy field above 35 T [14]. The lattice parameters of TbNiAl are close to the forbidden *c*/*a* ratio in the hexagonal ZrNiAl-type structure [16]. The temperature dependence of the lattice parameters then shows an abrupt transition around 100 K, keeping however the unit-cell volume unchanged. This structural transition has no significant impact on the magnetic properties [16]. Therefore, we did not investigate the MCE at temperatures around this structural transition and present measurements around and below T_N only. Both the entropy and temperature changes are evaluated from magnetization and specific heat data.

2. Experimental

Polycrystalline sample was prepared by arc-melting under an argon atmosphere from the stoichiometric mixture of pure elements (3 N for Tb and Ni, 5 N for Al). Sample was remelted several times to ensure the homogeneity. The TbNiAl single crystal was grown by Czochralski method from a 7 g melt of stoichiometric mixture of pure elements in a tri-arc furnace with a rotating water-cooled copper crucible under a protective argon atmosphere. The tungsten rod as a seed and 10 mm/h pulling speed were used. The Laue back-scattering patterns were used to check the single-crystalline state and to orient the crystal before cutting different pieces used in the measurement. The phase purity of the samples was verified by the X-ray powder diffraction.

Despite the relatively large number of studies using different experimental techniques, the specific heat of TbNiAl was not reported up to now. The structural transition observed in TbNiAl around 100 K [16] could be a reason. We have experienced that the thermal contact between the sample and the sample holder is usually strongly impaired when cooling below the transition. To avoid these difficulties with the structural transition, we have performed the heat capacity measurement with the sample covered on the bottom side by a Stycast epoxy. The Stycast coating does not affect the heat conduction to the sample significantly, as proved by numerous studies [17]. The heat capacity was determined using the relaxation method in a Quantum Design Physical Property Measurement System (PPMS) in temperature range from 4 to 70 K. The measurement was done on ~7.9 mg polycrystalline sample placed on ~0.94 mg of Stycast® 2850 FT. The heat capacity of the pure Stycast was then subtracted from the measured data.

The magnetization was measured on several samples. The single-crystal measurements were performed on a nearly cubic piece of 1.6 mm^3 oriented with the hexagonal *c*-axis parallel or perpendicular to the applied magnetic field. The measured data were corrected for the demagnetization field using the demagnetization factor of 0.3 that reflects the nearly cubic sample shape.

Further magnetization measurements were performed (i) on two bulk pieces (~6 mg) randomly cut from the polycrystalline sample, labeled P1 and P2 in further text, and (ii) on a fine powder sample with grains randomly fixed by a non-magnetic glue. The magnetization isotherms were measured using the PPMS equipment in the temperature range from 70 to 4 K in magnetic fields up to 2 and 5 T for the polycrystalline samples and single crystal, respectively.

3. Results and discussion

The magnetization isotherms measured on the single crystal with the hexagonal *c*-axis oriented along the magnetic field direction are plotted in Fig. 1. To reflect better the physical properties, the data presented in this figure are corrected for the demagnetization field. The metamagnetic transition to the ferromagnetic state at 4 K occurs around B_{crit} = 0.2 T. This value is smaller than previously published value of B_{crit} = 0.4 T [14], what can be ascribed to a certain sample dependence of this quantity. The value of B_{crit} decreases with increasing temperature, in agreement with previous results [14]. Above B_{crit}, the magnetization curves exhibit a slight increase, tending to reach 9μ_B/f.u. which is expected for Tb^{3+} ions. The magnetization isotherms measured on single crystal oriented with the *c*-axis perpendicular to the applied field are plotted in Fig. 2. We do not observe any metamagnetic transition up to 5 T and the magnetization in 5 T reaches 1.7μ_B/f.u. at 4 K what is in agreement with previously published data [14].

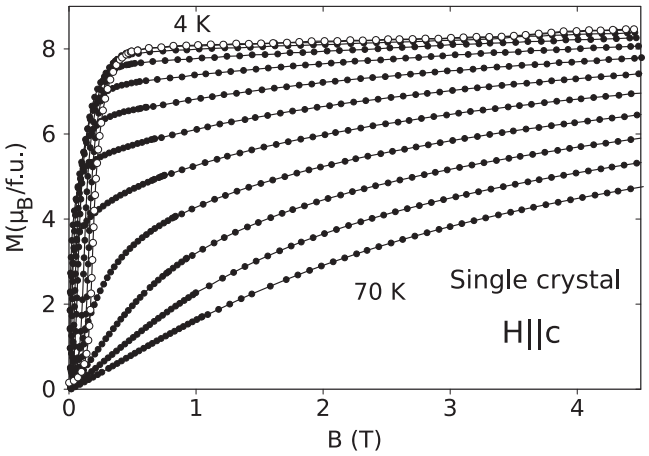

Fig. 1. The magnetization isotherms measured with the magnetic field applied parallel to the hexagonal *c*-axis of TbNiAl. The data measured at 4 K are shown as white circles to make the metamagnetic transition more visible. The demagnetization correction was applied (see text).

We should also mention, that the metamagnetic transition as observed in magnetization measurements presented in Refs. [11,14] as well as in our measurement shows significant hysteresis. The correctness of the entropy change evaluation in systems with hysteresis has been widely discussed in the last years [1,2,18–20]. The hysteresis is however observed only at low temperature in TbNiAl and therefore has no effect on evaluation of the entropy change where the MCE is significant in our case.

The entropy change ΔS was calculated from the magnetization isotherms (without demagnetization correction) by using equation derived from the Maxwell relation:

$$\Delta S_M(T_{av}, H_1) = \int_0^{H_1} \frac{M(T_{i+1}, H) - M(T_i, H)}{T_{i+1} - T_i} dH. \quad (1)$$

The entropy change calculated for the single crystal oriented with the *c*-axis parallel to the applied field is shown in Fig. 3 for several magnetic field changes. Negative values of ΔS in all presented magnetic field changes correspond with the ferromagnetic state that is established by the metamagnetic transition below 1 T. The maximum entropy change for the field change of 2 and 5 T reaches 8 and 15 J kg^{-1} K^{-1} at 49 K, respectively. The abrupt change of the slope of the $\Delta S(T)$ dependence occurs then below ~25 K what is presumably related to changes of magnetic structure below T_1. The entropy change of sample oriented perpendicular to the *c*-axis is plotted in Fig. 4. The values are near zero in the whole temperature

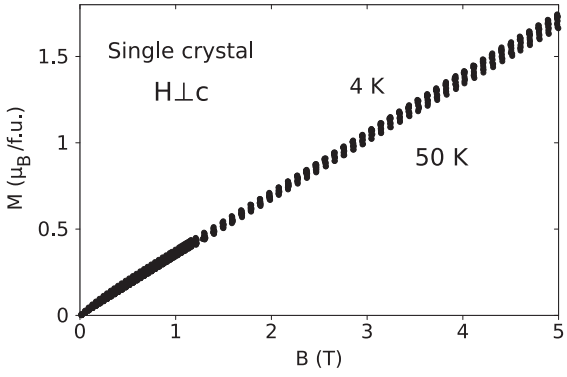

Fig. 2. The magnetization isotherms measured with the magnetic field applied perpendicular to the hexagonal *c*-axis of TbNiAl. The demagnetization correction was applied.

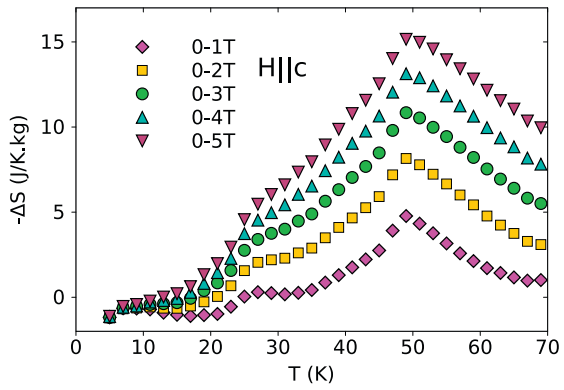

Fig. 3. The entropy change calculated from the magnetization isotherms for field applied parallel to the hexagonal *c*-axis of TbNiAl.

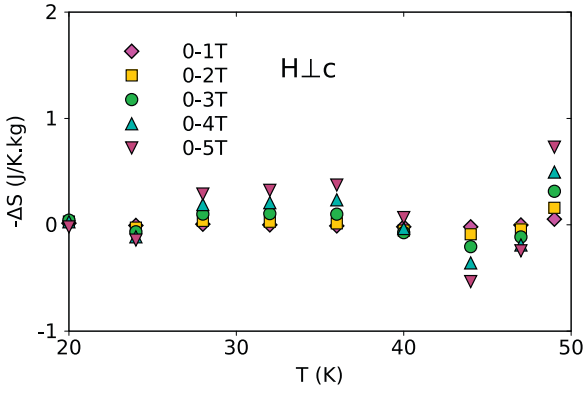

Fig. 4. The entropy change calculated from the magnetization isotherms for field applied perpendicular to the hexagonal *c*-axis of TbNiAl.

region as the antiferromagnetic structure remains almost intact by magnetic fields applied perpendicular to the *c*-axis.

The heat capacity of TbNiAl measured in zero magnetic field is plotted in Fig. 5. We observe two well pronounced anomalies with shape typical for a second-order phase transition. The transition temperatures of $T_N = 46$ K and $T_1 = 23$ K deduced from these data are in a good agreement with magnetization, susceptibility and neutron diffraction results [14,15]. To evaluate the temperature change, ΔT, due to MCE, the zero-field entropy of TbNiAl was determined by integrating the heat capacity data. The entropy in a certain magnetic field was then obtained as a sum of this zero-field entropy and the entropy change obtained from magnetization

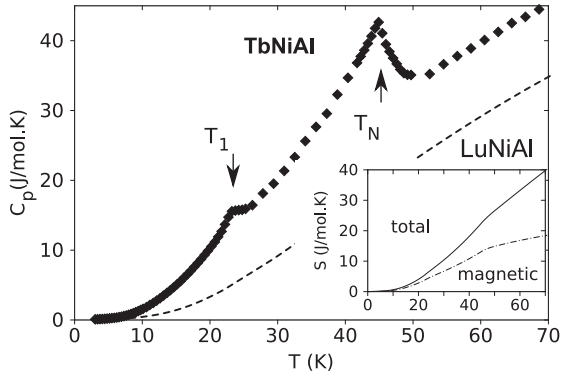

Fig. 5. The heat capacity of TbNiAl (full symbols) and of LuNiAl (dashed curve). The magnetic transitions at temperatures T_1 and T_N are clearly seen. The total and magnetic entropy of TbNiAl are shown in the inset.

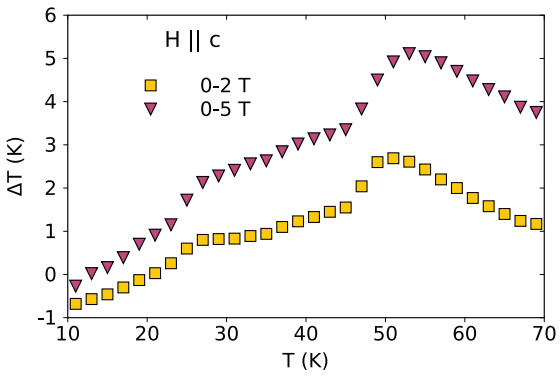

Fig. 6. The temperature change calculated from the zero-field heat capacity and the entropy change determined from magnetization data (see also Fig. 3).

data by the Maxwell equation (1). The temperature change was finally calculated as the difference between the temperatures at which the entropy in zero field and given magnetic field are equal. This way of estimating the temperature change accounts only the change due to the magnetic subsystem. However, our heat capacity measurements on the nonmagnetic analogues (YNiAl, LuNiAl) suggest that the contributions of the lattice and conducting electrons are not significant as the measurements in 0 and 5 T do not differ within experimental errors. The evaluated temperature change can be taken as a good estimate. The obtained ΔT vs T dependence for magnetic field applied along the *c*-axis is shown in Fig. 6. For field change of 5 T, the maximum temperature change of $\Delta T_{max} = 5$ K occurs at 53 K. The maximum of ΔT is at temperature, which is 4 K higher than the temperature of maximum of $|\Delta S|$. This is due to the fact that the temperature change strongly depends also on the heat capacity curve $C_p(T)$ (see Fig. 5). The same entropy change results in a larger temperature change when the heat capacity and hence the slope of the $S(T)$ curve is smaller. The temperature change at temperatures between T_N and T_1 for field change of 2 T has a plateau-like character. The temperature change at temperatures between T_N and T_1 for field change of 5 T very slowly decrease with decreasing temperature. The slope of the ΔT vs T curve is abruptly changed at T_1 and ΔT quickly drops to zero for both field changes. Let us now turn to polycrystalline samples. Previous study of MCE in polycrystalline TbNiAl [11] revealed the entropy change surprisingly only slightly smaller than our present results obtained for the easy magnetization direction $H||c$. We have performed magnetization measurements on several types and pieces of polycrystalline samples as described above. The measured magnetization curves (see Fig. 7) show striking difference between the fixed powder and

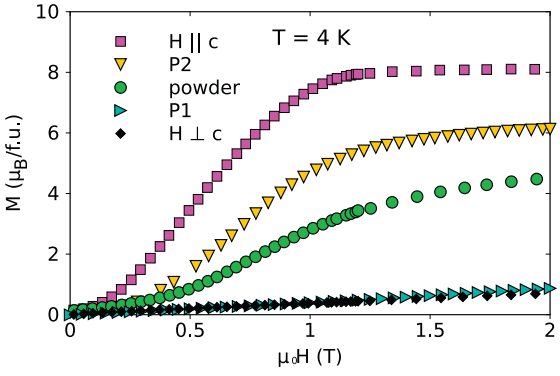

Fig. 7. The comparison of magnetization measured on different samples at 4 K. The measurement on single crystal with orientation of the *c*-axis parallel and perpendicular to the magnetic field, the fixed powder and two pieces randomly cut from the as-cast ingot (see text).

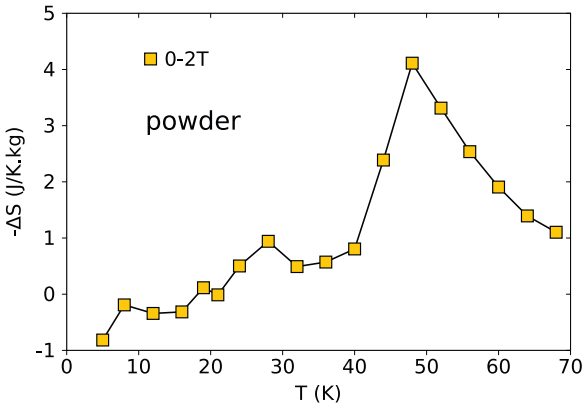

Fig. 8. The entropy change calculated from the magnetization isotherms measured on the fixed powder for a field change of 2 T. The curve has a similar shape as measured on the single crystal, however, the maximum value is almost a half of the value obtained on the single crystal.

bulk pieces as well as between different bulk pieces, presumably due to strong texture present in the bulk pieces. The magnetization curves of the randomly oriented powder are similar to those published in the previous studies [15,16,22] except for data in Ref. [11] which resemble more the easy-axis single-crystal data. As the sample form is not described in Ref. [11], we tend to assume that the data were obtained on a free powder or a bulk piece with a strong texture similar to our P2 sample.

The entropy change determined from magnetization curves measured on the fixed powder which should represent an ideal polycrystal is plotted in Fig. 8. It shows similar character as that obtained on the single crystal for $H||c$ but the values are substantially reduced. The maximum entropy change for field change of 2 T reaches $-4.1\,J\,kg^{-1}\,K^{-1}$ at 49 K. The corresponding value of $\Delta S_{max} = -8.2\,J\,kg^{-1}\,K^{-1}$ measured for single crystal thus represents 100% increase compared to this ideal polycrystal which is much more than 40% increase found in DyNiAl [13].

The relative cooling power, RCP, calculated as the product of ΔS_{max} and the full width at half maximum of the ΔS vs T plot, is another quantity used when comparing different magnetocaloric materials. We can roughly estimate the RCP values of TbNiAl single crystal with field applied along c-axis to be 190 and 630 J kg^{-1} for the 2 and 5 T change, respectively. The RCP value of 70 J kg^{-1} can be estimated for polycrystalline TbNiAl and 2 T field change.

Our results revealed a strongly anisotropic MCE in TbNiAl. The single-crystal magnetocaloric characteristics show 100% increase compared to an ideal polycrystal. Furthermore, we have found that the magnetic and magnetocaloric phenomena measured on several bulk "polycrystalline" pieces are rather different. These small bulk pieces presumably contain large singlecrystalline grains or exhibit large texture. The measured data are then close to results obtained on the single crystal. This can occur in any anisotropic material and should not be forgotten when evaluating "polycrystalline" data measured on a bulk. It could be also of importance when designing real cooling matrices.

The magnetocaloric effect of TbNiAl is well comparable with other materials considered as good magnetic refrigerants. For example, the RCP values for 5 T field change of Gd, $Gd_5Si_2Ge_2$ or $MnFeP_{0.45}As_{0.55}$ lie in the range between 400 and 600 J kg^{-1} [23–25]. TbNiAl can also be compared with the materials which exhibit the MCE in the same temperature range. DyNi reaches the maximum value of $\Delta S_{max} = 12.5\,J\,kg^{-1}\,K^{-1}$ at 60 K [26] and the corresponding RCP = 375 J kg^{-1} for the field change of 5 T. ΔS_{max} in $DyAl_2$ reaches about 19 J kg^{-1} k^{-1} around 60 K for the field change of 5 T [27]. Measurements of the isostructural DyNiAl single-crystal revealed $\Delta S_{max} = 22\,J\,kg^{-1}\,K^{-1}$ at 30 K for field change of 5 T when direction of the field is parallel to the hexagonal c-axis [13]. DyCuAl is also isostructural to the TbNiAl and undergoes magnetic phase transition at 28 K. The maximum entropy change of 10.9 and 20.4 J kg^{-1} K^{-1} for field change of 2 and 5 T, respectively, was reported [27]. The ordering temperature in $Gd_{1-x}Sm_xMn_2Si_2$ with $x = 0.6$ was found to be 48 K and the maximum entropy change is 0.9 and 1.6 J kg^{-1} K^{-1} for a field change of 2 and 5 T, respectively [28].

4. Conclusions

Magnetization and specific heat measurements performed on single crystal revealed strongly anisotropic magnetocaloric effect in TbNiAl which orders antiferromagnetically below $T_N = 47$ K and undergoes metamagnetic transition to ferromagnetic state in fields below 1 T. The large MCE occurs for field applied along the hexagonal c-axis whereas the entropy change is almost zero for the perpendicular field direction. The easy-axis magnetocaloric characteristics show 100% increase compared to an ideal polycrystal. We have found also huge differences between several bulk polycrystalline pieces due to presence of large crystal grains or sample texture.

Acknowledgements

The work was supported by the Grant Agency of the Czech Republic under the Grant No. 106/09/0030 and 202/08/0711, the work of J.K. was also supported by the grant SVV-2010-261303. This work is a part of the research program MSM 0021620834 financed by the Ministry of Education of the Czech Republic.

References

[1] N.A. de Oliveira, P.J. von Ranke, Phys. Rep. 489 (2010) 89.
[2] A.M. Tishin, Y.I. Spichkin, The Magnetocaloric Effect and Its Applications, Institute of Physics, Bristol, 2003.
[3] M. Zou, Y. Mudryk, V. Pecharsky, K. Gschneidner, D. Schlagel, T. Lograsso, Phys. Rev. B 75 (2007) 024418.
[4] A.L. Lima, K.A. Gschneidner Jr., V.K. Pecharsky, J. Appl. Phys. 96 (2004) 2164.
[5] A.L. Lima, A.O. Tsokol, K.A. Gschneidner Jr., V.K. Pecharsky, T.A. Lograsso, D.L. Schlagel, Phys. Rev. B 72 (2005) 024403.
[6] D.X. Li, S. Nimori, T. Shikama, Solid State Commun. 150 (2010) 1865.
[7] S. Majumdar, E.V. Sampathkumaran, P.L. Paulose, H. Bitterlich, W. Löser, G. Behr, Phys. Rev. B 62 (2000) 14207.
[8] B.J. Korte, V.K. Pecharsky, K.A. Gschneidner Jr., J. Appl. Phys. 84 (1998) 5677.
[9] N.K. Singh, K.G. Suresh, R. Nirmala, A.K. Nigam, S.K. Malik, J. Appl. Phys. 99 (2006) 08K904.
[10] N.K. Singh, K.G. Suresh, R. Nirmala, A.K. Nigam, S.K. Malik, J. Appl. Phys. 101 (2007) 093904.
[11] N.K. Singh, K.G. Suresh, R. Nirmala, A.K. Nigam, S.K. Malik, J. Magn. Magn. Mater. 302 (2006) 302.
[12] V. Sechovský, L. Havela, in: K.H.J. Buschow (Ed.), Handbook of Magnetic Materials, vol. 1, Elsevier Science B.V., Amsterdam, 1998, pp. 1–289.
[13] J. Kaštil, P. Javorský, A.V. Andreev, J. Magn. Magn. Mater. 321 (2009) 2318.
[14] P. Javorský, P. Burlet, V. Sechovský, A.V. Andreev, J. Brown, P. Svoboda, J. Magn. Magn. Mater. 166 (1997) 133.
[15] G. Ehlers, H. Maletta, Z. Phys. B 99 (1996) 145.
[16] J. Prchal, P. Javorský, J. Rusz, F. de Boer, M. Diviš, H. Kitazawa, A. Dönni, S. Daniš, V. Sechovský, Phys. Rev. B 77 (2008) 134106, and references therein.
[17] P. Javorský, F. Wastin, E. Colineau, J. Rebizant, P. Boulet, G. Stewart, J. Nucl. Mater. 344 (2005) 50.
[18] J. Kamard, J. Kaštil, Z. Arnold, P. Javorský, V. Sechovský, Acta Phys. Pol. A 118 (2010) 1000.
[19] V. Basso, C.P. Sasso, M. LoBue, J. Magn. Magn. Mater. 316 (2007) 262.
[20] J.S. Amaral, V.S. Amaral, Appl. Phys. Lett. 94 (2009) 042506.
[22] G. Ehlers, C. Ritter, A. Kurtjakow, W. Miekeley, N. Stüsser, Th. Zeiske, H. Maletta, Phys. Rev. B 59 (1999) 8821.
[23] O. Tegus, E. Brück, K.H.J. Buschow, F.R. de Boer, Nature 415 (2002) 150.
[24] M.H. Phan, S.C. Yu, J. Magn. Magn. Mater. 308 (2007) 325.
[25] P.W. Egolf, Proceedings of the First International Conference on Magnetic Refrigeration near Room Temperature, Montreux, Switzerland, 2005.
[26] S.K. Tripathy, K.G. Suresh, R. Nirmala, A.K. Nigam, S.K. Malik, Solid State Commun. 134 (2005) 323.
[27] Q.Y. Dong, B.G. Shen, J. Chen, J. Shen, J.R. Sun, J. Appl. Phys. 105 (2009) 113902.
[28] P. Kumar, N.K. Singh, K.G. Suresh, A.K. Nigam, J. Alloys Compd. 427 (2007) 42.